

## Stiffness, workspace and dynamic performance analysis of 4UPS-PU mechanism

Wei Bin

**Summary.** This paper focuses on the stiffness, workspace and dynamic performance analysis of 4UPS-PU manipulator. Firstly, the inverse kinematic and Jacobian matrix of the mechanism are analysed and the global stiffness as well as its optimization using Genetic algorithm (GA) are investigated as to obtain the optimal stiffness in each direction. Secondly, the workspace of the mechanism is optimized by maximizing the global condition index which derived based on Monte Carlo method to have the well-conditioned workspace without having the undesirable kinematic characteristics and the well-conditioned workspace of the mechanism is plotted. Lastly, two dynamic performance indexes, which are the driving force index and loading capacity index, are proposed to analyse the dynamic performance of the mechanism.

*Key words:* parallel manipulator, stiffness, workspace, dynamic performance, optimization

### Introduction

Parallel manipulators have been widely used during the past decade, such as parallel robotic machine tools [1], micro-instruments [1], medical purposes [2-4], automotive industries[5], etc, due to the merits that parallel manipulators instinctively possess, like high stiffness, low inertia, good acceleration, load distribution, etc. However, the major drawback of the parallel manipulators is their limited workspace.

Stiffness is the measurement of the ability of a body to resist deformation due to the action of external forces. In many applications, stiffness is a critical important factor for parallel manipulators since it relates to accurate positioning and other dynamic performances. Stiffness analysis on manipulators has been the subject of many robotic researchers during the past few years. L.W. Tsai [6, 7] has studied the stiffness properties of the 3-DOF position mechanisms for use in the hybrid kinematic machines. D. Zhang and Gosselin [8, 9] have studied the stiffness and compliance of a series of N-DOF parallel manipulators based on the kinetostatic model by considering compliance of the central passive limb. Other researchers [10] have studied the stiffness of the 3-PUU parallel kinematic machine, etc. Here the global stiffness and its optimization of 4UPS-PU mechanism are investigated in order to obtain the optimal stiffness in each direction. Note that U represents the Hooke joint, P represents the prismatic joint and S represents the spherical joint.

Workspace is a common factor to evaluate the performance of parallel manipulators. Some authors described the workspace of a parallel mechanism by

discretizing the Cartesian workspace [11]. Some scholars considered the constraints exerted by link length, joint angle limitations and link interference to search the workspace of parallel manipulators [12]. Others also used the CAD, Matlab Simulink as well as Cosmosmotion to plot the workspace of the parallel manipulators [13]. In this paper, the interference of each leg is neglected and only considering the length limit of each actuated leg as well as the joints' range that located at the central passive leg [14]. A parallel manipulator designed for maximum workspace volume may not be the optimal design for practical applications which probably would result in undesirable kinematic characteristics like poor dexterity. Here the global condition index is used to evaluate the workspace of the mechanism and the workspace of the mechanism is optimized by maximizing the global condition index to have the well-conditioned workspace. Furthermore, dynamic performance is another critical important factor to evaluate the performances of parallel manipulators as a whole. Here the driving force and loading capacity index are proposed to evaluate the performances of the mechanism.

### Geometric description of 4UPS-PU mechanism

As represented in Figure 1, the spatial 3-DOF mechanism consists of five kinematic chains, including four variable length legs with identical topology and one passive constraining leg. In this 3-DOF parallel manipulator, the kinematic chains associated with the four identical legs consist of a fixed Hooke joint U, a moving link, an actuated prismatic joint P, another moving link and a spherical joint S attached to the platform from base to platform. The fifth chain connecting the base centre to the platform center is a passive constraining leg and has a different architecture from the other four identical legs. It consists of a prismatic joint attached to the base, a moving link and a Hooke joint attached to the platform. The central leg is used to restrict the moving platform from moving along  $X$ ,  $Y$  axis and rotation about  $Z$  axis, which makes the mechanism to be only three degrees of freedom. For the purpose of analysis, a fixed reference frame ( $XYZ$ ) is attached to the center of the base at point  $O$ . The angle between  $b_i$  and  $X$ -axis is defined as  $\varphi_i$ . A moving frame ( $xyz$ ) is attached to the center of the moving platform at point  $O_e$ . The angle between  $a_i$  and  $x$ -axis is defined  $\varphi_i'$ . Here we assume  $\varphi_i' = \varphi_i$ .

### Kinematic analysis

From Fig.1 we can see that

$$b_i + l_i = a_i + p_e = Qa_i' + p_e \quad (1)$$

where  $l_i$  is the vector of each actuated leg,  $a_i'$  and  $b_i$  are the position vectors of points  $P_i$  and  $B_i$  with respect to the moving frame and fixed frame, respectively.  $Q$  is the rotation matrix of moving platform with respect to the fixed base,  $p_e$  is the vector  $OO_e$ .

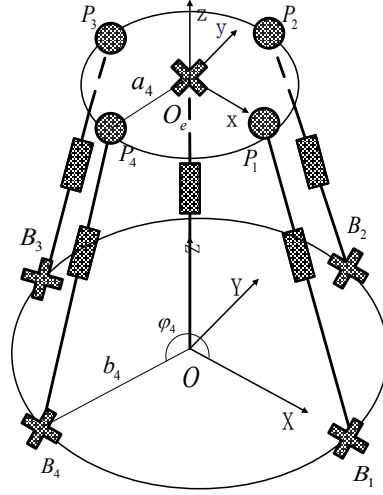


Fig.1. Schematic representation of the 4UPS-PU mechanism

$$a'_i = [r \cos \varphi_i \quad r \sin \varphi_i \quad 0]^T \quad (i=1, 2, 3, 4),$$

$$b_i = [R \cos \varphi_i \quad R \sin \varphi_i \quad 0]^T \quad (i=1, 2, 3, 4),$$

$$p_e = [0 \quad 0 \quad h]^T,$$

where  $r$  and  $R$  are the radii of the moving platform and fixed base, respectively. The kinematic structure of the passive constraining leg is shown in figure 2. From figure 2, one can obtain the D-H parameters given in table 1.

Let  $\theta_2$  and  $\theta_3$  be the joint angles of the Hooke joint in the central passive leg. We take the Cartesian coordinate frame as frame 0, and define  $\alpha_0 = 0^\circ$ ,  $\theta_0 = 0^\circ$ , then one has the following

$$Q_0 = \begin{bmatrix} 1 & 0 & 0 \\ 0 & 1 & 0 \\ 0 & 0 & 1 \end{bmatrix},$$

where  $Q_0$  is the rotation matrix from the fixed reference frame to the first frame of the central passive constraining leg,  $Q_1$  is the rotation matrix from the first frame to the second frame of the central passive constraining leg,  $Q_2$  is the rotation matrix from the second frame to the third frame of the central passive constraining leg,  $Q_3$  is the rotation matrix from the third frame to the last frame of the central passive constraining leg.

$$Q_1 = \begin{bmatrix} 0 & 0 & 1 \\ 1 & 0 & 0 \\ 0 & 1 & 0 \end{bmatrix} \quad Q_2 = \begin{bmatrix} \cos \theta_2 & 0 & \sin \theta_2 \\ \sin \theta_2 & 0 & -\cos \theta_2 \\ 0 & 1 & 0 \end{bmatrix} \quad Q_3 = \begin{bmatrix} \cos \theta_3 & 0 & -\sin \theta_3 \\ \sin \theta_3 & 0 & \cos \theta_3 \\ 0 & -1 & 0 \end{bmatrix}.$$

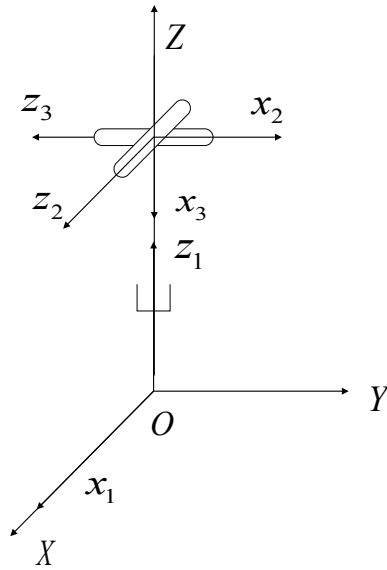


Fig. 2. The kinematic structure of the passive constraining leg

Table 1. The D-H parameters for the passive constraining leg

$i$	$a_i$	$d_i$	$\alpha_i$	$\theta_i$
0	0	0	0	0
1	0	$h$	$90^\circ$	$90^\circ$
2	0	0	$90^\circ$	$\theta_2$
3	0	0	$-90^\circ$	$\theta_3$

So the rotation matrix of the moving frame with respect to the fixed frame can be expressed as  $Q = Q_0 Q_1 Q_2 Q_3$ . The vector  $l_i$  can be written from eq. (1) as

$$l_i = p_e + a_i - b_i. \quad (2)$$

The length of the  $i^{\text{th}}$  leg is written as

$$q_i^2 = \|l_i\|^2 = l_i^T l_i. \quad (3)$$

Hence we completed the inverse kinematics analysis of the manipulator. The Jacobian matrix maps the output velocity to the input velocity. The Jacobian matrix for the manipulator can be determined by time differentiating equation (3) as follows,

$$B \dot{q} = A \dot{t}, \quad (4)$$

$$J = B^{-1} A, \quad (5)$$

where

$$A = \begin{bmatrix} a_{11} & a_{12} & a_{13} \\ a_{21} & a_{22} & a_{23} \\ a_{31} & a_{32} & a_{33} \\ a_{41} & a_{42} & a_{43} \end{bmatrix}, \quad B = \begin{bmatrix} q_1 & 0 & 0 & 0 \\ 0 & q_2 & 0 & 0 \\ 0 & 0 & q_3 & 0 \\ 0 & 0 & 0 & q_4 \end{bmatrix}, \quad t = \begin{bmatrix} \dot{\theta}_2 \\ \dot{\theta}_3 \\ \dot{h} \end{bmatrix},$$

$$\begin{aligned} a_{i1} &= Rr \cos^2 \varphi_i \sin \theta_1 \cos \theta_2 + Rr \cos \varphi_i \sin \varphi_i \cos \theta_1 + hr \cos \varphi_i \cos \theta_1 \cos \theta_2 - hr \sin \theta_1 \sin \varphi_i, \\ a_{i2} &= Rr \cos^2 \varphi_i \cos \theta_1 \sin \theta_2 + Rr \sin \varphi_i \cos \varphi_i \cos \theta_2 - hr \cos \varphi_i \sin \theta_1 \sin \theta_2, \\ a_{i3} &= h + r \sin \theta_1 \cos \theta_2 \cos \varphi_i + r \cos \theta_1 \sin \varphi_i \quad (i=1,2,3,4). \end{aligned}$$

## Stiffness optimization of 4ups-pu mechanism

### Global stiffness of the manipulator

When a manipulator performs a given task, the end-effector exerts force onto its environment. The reaction force will cause the end-effector to be deflected away from its desired location. Intuitively, the amount of deflection is a function of the applied force and the stiffness of the manipulator. Thus, the stiffness of a manipulator has a direct impact on its position accuracy.

Let  $F$  denote a 3-dimensional vector of end effector output forces and  $\Delta x$  represent a 3-dimensional vector of displacement of the end effector. It can be shown that:

$$F = K \Delta x, \quad (6)$$

where

$$K = J^T K_J J \quad (7)$$

is known as the stiffness matrix, and  $K_J$  is a  $4 \times 4$  diagonal matrix in which each non-zero diagonal element  $k_i$  represents the stiffness constant of the  $i$ th joint actuator. Furthermore, if  $k_1 = k_2 = k_3 = k_4 = k$ , the above equation reduces to

$$K = k J^T J. \quad (8)$$

The stiffness of the manipulator is expressed by a  $3 \times 3$  matrix. The diagonal element of the matrix is the manipulator's pure stiffness in each direction. The sum of leading diagonal elements of the stiffness matrix is defined as the global stiffness [15]. Stiffness is a critical important factor for parallel manipulators since high stiffness can lead to high precision. Specifically, global stiffness  $K_{global}$  as stated in equation (9) is related to system rigidity [16]. Here we optimize the global stiffness of the mechanism in order to obtain the optimal stiffness in each direction:

$$K_{global} = \eta_1 k_{11} + \eta_2 k_{22} + \eta_3 k_{33}, \quad (9)$$

where  $k_{ii}$  ( $i=1,2,3$ ) denotes the diagonal elements of the manipulator's stiffness matrix and  $\eta_i$  is the weight factor for each directional stiffness, which characterizes the priority of the stiffness in this direction. This would maximize the sum of the

diagonal elements which is the global stiffness. Although we could not maximize each diagonal element individually, we can always optimize each stiffness by distributing the weighting factors.

For the purpose of numerical analysis, we assume  $h=0.66$  m,  $\theta_2 = -90^\circ$ ,  $\theta_3 = 90^\circ$ ,  $\eta_i = 1$ , the design variables are  $r$  and  $R$ , their bound are  $r \in [0.03, 0.13]m$  and  $R \in [0.08, 0.18]m$  according to the practical requirements. Then we can obtain  $K_{global}$  stiffness distribution as shown in Fig. 3. Similarly when we assume  $h=0.36$  m,  $\theta_2 = -90^\circ$ ,  $\theta_3 = 90^\circ$ ,  $\eta_i = 1$ , the global stiffness  $K_{global}$  distribution is shown in Fig. 4. Figure 5 is the  $K_{global}$  distribution comparison between above two scenarios. When the design variables are  $\theta_2 \in [-120^\circ, -60^\circ]$  and  $\theta_3 \in [60^\circ, 120^\circ]$ , and assuming  $r=0.11$  m,  $R=0.16$  m,  $h=0.66$  m,  $\eta_i = 1$ , one can also have the  $K_{global}$  distribution in figure 6. Through different experiments we found that  $r, R, h, \theta_2, \theta_3$  affect the  $K_{global}$ .

Next, we need to determine the values of  $r, R, h, \theta_2$  and  $\theta_3$  simultaneously that lead to the maximum  $K_{global}$ .

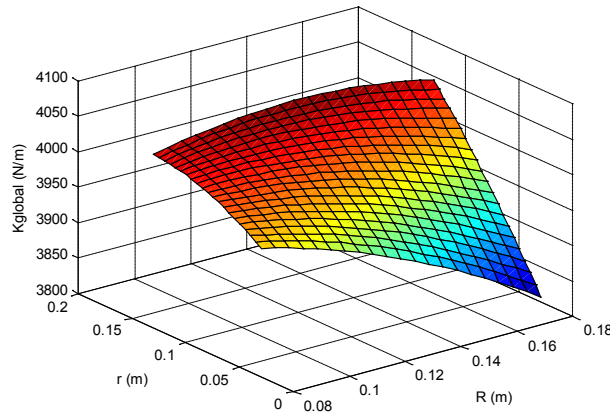


Fig.3.  $K_{global}$  distribution when  $h=0.66m$ ,  $\theta_2 = -90^\circ$ ,  $\theta_3 = 90^\circ$ .

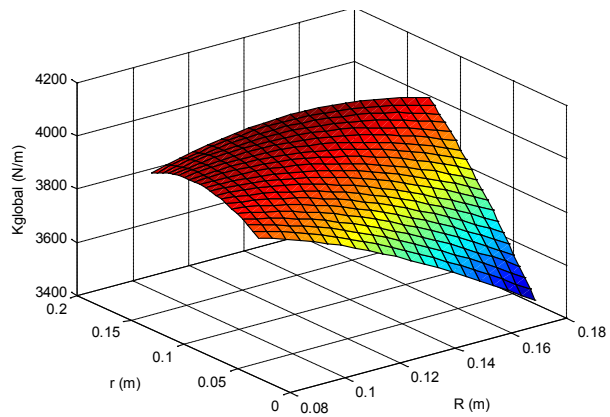


Fig.4.  $K_{global}$  distribution when  $h=0.36m$ ,  $\theta_2 = -90^\circ$ ,  $\theta_3 = 90^\circ$ .

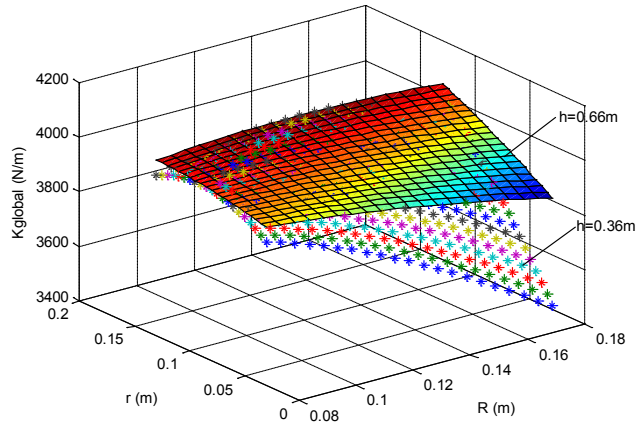


Fig.5.  $K_{global}$  distribution when  $\theta_2 = -90^\circ$ ,  $\theta_3 = 90^\circ$ .

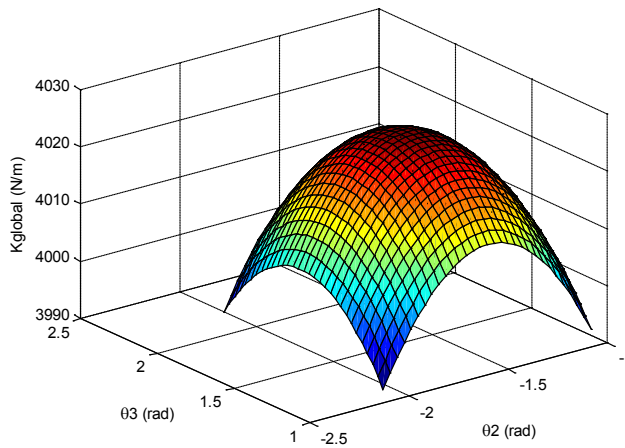


Fig.6.  $K_{global}$  distribution when  $h = 0.66$  m,  $r = 0.11$  m,  $R = 0.16$  m.

### Genetic Algorithms

Genetic algorithm (GA) is based on the natural selection and it repeatedly modified a population of individual solutions. At each step, the GA selects individuals at random from the current population to be parents and use them produce the children for the next generations. From generations to generations, the population is going toward an optimal solution.

Traditional optimization methods use a local search by a convergent stepwise procedure, which compares the values of the next points and then moves to the optimal points. Global optima can be found only if the problem has certain convexity properties which guarantee any local optima is a global optimum. It has the danger of falling in local optima. However, genetic algorithms are based on the population-to-population rule; it can escape from local optima [1]. Genetic algorithms have the advantages of good convergence and robustness properties: such as the following.

- (1) They require no knowledge or gradient information about the optimization problems; they can solve any kind of objective functions and any kind of constraints defined on discrete, continuous or mixed search spaces.
- (2) Discontinuities present on the optimization problems has little effect on the overall optimization performance.
- (3) It is effective at performing global search instead of local optima.
- (4) It performs very well for large-scale optimization problems.
- (5) They can be employed for wide variety of optimization problems.

Here, the genetic algorithm is used to optimize the global stiffness  $K_{global}$  of the 4UPS-PU manipulator. Our objective function is:  $K_{global} = \eta_1 k_{11} + \eta_2 k_{22} + \eta_3 k_{33}$ , and our goal is to maximize  $K_{global}$ . Note that the optimization functions in the GA minimize the objective function, in order to maximize the objective function, we need to minimize  $-K_{global}$ , because the point at which the minimum of  $-K_{global}$  occurs is the same as the point at which the maximum of  $K_{global}$  occurs. The design variables are  $r, R, h, \theta_2$  and  $\theta_3$ . Their bounds are the following according to practical requirements,  $r \in [0.03, 0.13]$  m,  $R \in [0.08, 0.18]$  m,  $h \in [0.5, 0.7]$  m,  $\theta_2 \in [-120^\circ, -60^\circ]$ ,  $\theta_3 \in [60^\circ, 120^\circ]$ . Some genetic parameters and operators are set as: scaling function = rank; selection function = roulette; crossover function = intermediate; crossover ratio = 1.0; mutation function = adaptive feasible; population size = 20; maximum number of generations = 100.

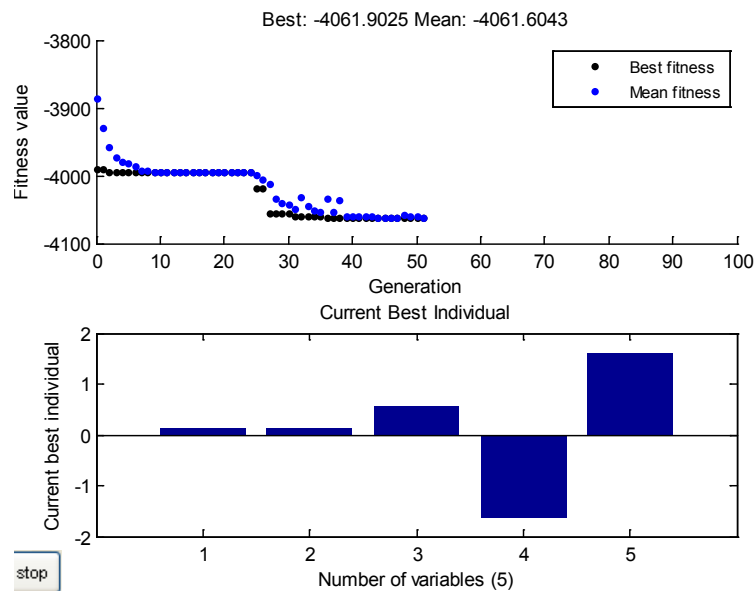


Fig. 7. The best fitness value and the best individuals of the global stiffness optimization

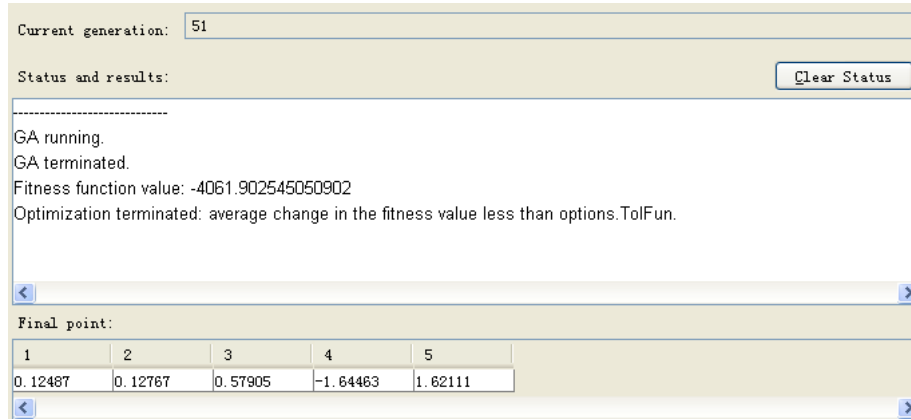


Fig. 8. The results of the global stiffness optimization

The Fig.7 displays a plot of the best function values in each generation versus iteration number. The black points denote the best fitness values and the blue points denote the mean fitness values in each generation. The plot also displays the current best individuals. The optimal parameters are obtained after 51 generations as follows:

$$[r, R, h, \theta_2, \theta_3] = [0.12487\text{m}, 0.12767\text{m}, 0.57905\text{m}, -1.64463 \text{ rad}, 1.62111 \text{ rad}]$$

And the maximum of  $K_{global}$  is 4061.9025 N/m.

The results of the global stiffness optimization are shown in Figure 8. The results suggest that in order to make the global stiffness of the manipulator reach the maximum, the radius of the moving platform should be 0.125m, the heave of the manipulator should be 0.579m, the radius of the base should be 0.128m,  $\theta_2 = -1.645\text{rad}$  and  $\theta_3 = 1.621\text{rad}$ .

## Workspace analysis and optimization

Parallel mechanisms have the merit of high stiffness, high loading capacity, etc, but the disadvantage of parallel mechanisms is the limited workspace as compare to their serial counterparts. So we need to maximize the workspace to make it bigger, but parallel mechanisms designed for maximum workspace volume may not be the optimal design for practical applications which probably will lead to poor dexterity. Some proposed the global condition index [17] to optimize the workspace of a mechanism to avoid the undesirable kinematic characteristics like poor dexterity. Here the global condition index is used to evaluate the workspace of the mechanism to have the well-conditioned workspace. The global condition index is defined as follows

$$\eta = \int_w \frac{1}{k} dW \quad (10)$$

where  $k$  is the condition number of the Jacobian of the manipulator at a given position in the workspace. The global condition index is a performance index which shows how far the mechanism from singularity is. Analytical solution to equation (10) is difficult to obtain, therefore we have to use a numerical solution technique like Monte Carlo

method. The details of the method are as follows: first of all, many points  $n_{total}$  are randomly selected in the possible workspace which is defined for this mechanism as follows:  $-120^\circ \leq \theta_2 \leq -60^\circ$ ,  $60^\circ \leq \theta_3 \leq 120^\circ$ ,  $0.5 \leq h \leq 0.7$ ; secondly, we need to check whether each point falls within the workspace of the mechanism or not, this can be done through solving inverse kinematic for each leg to see whether the leg length satisfies the leg limits which we assume the leg limits is  $0.6 \leq q_i \leq 0.9$ ; thirdly, determine the kinematics condition index which is the summation of reciprocal of the condition number for every point falling in the workspace of the mechanism; finally, the global condition index is derived through multiplying the kinematics condition index and volume of the possible workspace, after that dividing by the number of points we previously selected, then we obtain the following:

$$\eta = \frac{\pi r^2 (h_1 - h_2) \cdot \sum_i \frac{1}{k_i}}{n_{total}}$$

Where  $h_1$  is the maximum height of points  $P_i$  with respect to  $O$ ,  $h_2$  is the minimum height of points  $P_i$  with respect to  $O$ . The design variables considered are  $r, R, \varphi_2, \varphi_3, \varphi_4$ . In order to bound the solution and ensure a practical realization, the objective function is subject to the following constraints:

(1)  $r \in [0.03, 0.13]$  m,  $R \in [0.08, 0.18]$  m,  $\varphi_2 \in [0, 2\pi]$ ,  $\varphi_3 \in [0, 2\pi]$ ,  $\varphi_4 \in [0, 2\pi]$ ; (2) each leg must have an angular separation of at least  $5^\circ$  from each of the other legs. Now our objective function is

$$\eta = \frac{\pi r^2 (h_1 - h_2) \cdot \sum_i \frac{1}{k_i}}{n_{total}}$$

Given this problem formulation, the optimization is computed using the Matlab optimization toolbox and produced the results as follows:  $R=0.08$ ,  $r=0.03$ ,  $\varphi_2=1.519rad$ ,  $\varphi_3=3.121rad$ ,  $\varphi_4=4.652rad$  when 1000 points were used for the Monte Carlo method.

Here we neglect the interference of each leg and only consider the length limits of each actuated leg as well as the joints' range that located at the central passive leg<sup>[14]</sup>. The searching procedure is stated as follows: first of all, we select a certain value (from bottom value to top value to search) of  $\theta_2$ ,  $\theta_3$  and  $h$  in their confined bounds, then solve the inverse kinematic which is the length of each actuated leg, if the leg length is within the leg length limit  $0.6 \leq q_i \leq 0.9$ , then the center point of the moving platform is within the workspace, otherwise it is not. The workspace of parallel mechanism is a set to which a point on the moving platform can reach. For the purpose of showing the workspace more clearly, we select 36 boundary points located on the moving platform; the surrounded area subject to the trace of the 36 points with respect to the fixed frame is the workspace of this mechanism. The workspace is the following:

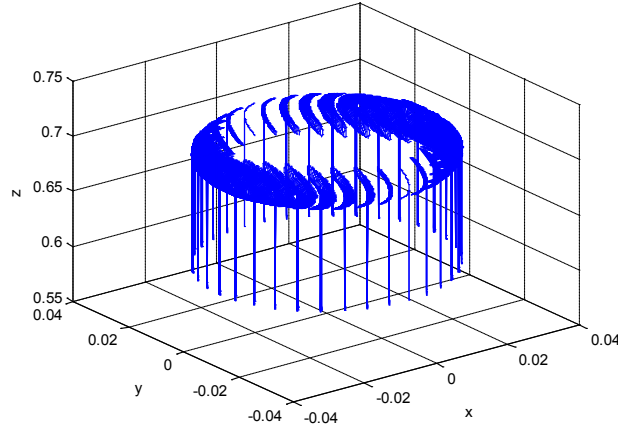


Fig. 9. The well-conditioned workspace of 4UPS-PU mechanism

## Dynamic performance

Dynamic performances are the basis for the dynamic analysis and design. The loading capacity index and driving force index are proposed to analyze the dynamic performances of the 4UPS-PU mechanism.

### *Loading capacity index*

Loading capacity is an important factor to evaluate the dynamic performance of the mechanism. Due to the fact that the generalized force exerted on the end effector has to do with the Jacobian matrix of the mechanism, the generalized force will change along with the change of the position and orientation of the mechanism. Here we define the actuator force of the mechanism  $f$  and the external force or torque exerted on the end effector  $F$ , one can have the following

$$F = G \cdot f, \quad (11)$$

where  $G$  is the force Jacobian matrix. We have the following equation from the dual relationship between motion transmission and force transmission of the mechanics:

$$G = J^T. \quad (12)$$

Here we define the extreme value of the norm of output force or torque  $F$  to be the loading capacity index when the norm of the actuator force is unit one to analyze the loading capacity of the mechanism [18]. In order to derive the extreme value, we make the Lagrangian equation as follows

$$L_f = f^T G^T G f - \lambda_F (f^T f - 1), \quad (13)$$

where  $\lambda_F$  is the Lagrangian multiplier.

When  $\|f\| = 1$ , the extreme value is the square root of the maximum and minimum eigenvalue of matrix  $G^T G$ ,

$$\|F\|_{\max} = \sqrt{\lambda_1(G^T G)} = \sigma_1(G), \quad (14)$$

$$\|F\|_{\min} = \sqrt{\lambda_2(G^T G)} = \sigma_2(G), \quad (15)$$

where  $\lambda_1(G^T G)$  and  $\lambda_2(G^T G)$  are the maximum and minimum eigenvalue of the matrix  $G^T G$ , respectively.  $\sigma_1(G)$  and  $\sigma_2(G)$  are the maximum and minimum singular value of matrix  $G$ .  $\|F\|_{\max}$  and  $\|F\|_{\min}$  are the maximum and minimum loading capacity when the norm of the vector of actuator force  $f$  is unit one. Here we propose the maximum loading capacity as the loading capacity index to evaluate the loading performance of the mechanism. The more the index is, the better performance of the mechanism has. Figure 10 shows the typical loading capacity index distribution when  $h$  is 0.6 m and the radii of the base and moving platform are 0.08 m and 0.03 m as a case. Through many experiments, one can find that the loading capacity index ranges slightly in the workspace and properly distributed. The index doesn't change dramatically while the moving platform changes. It indicates that the mechanism has good stability.

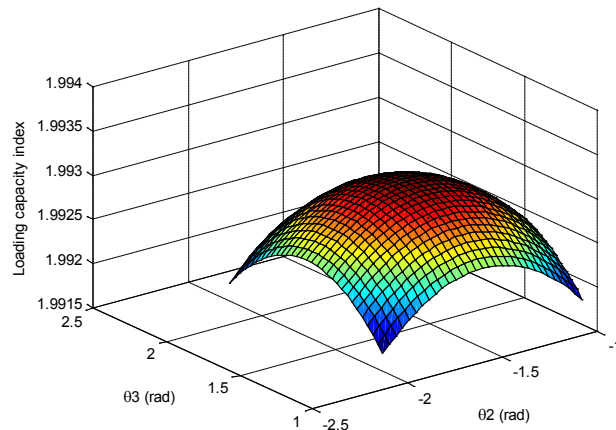


Fig. 10. Loading capacity index distribution

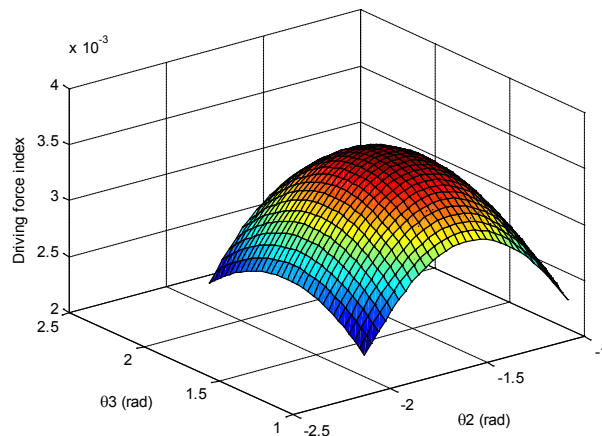


Fig. 11. Driving force index distribution

### Driving force index

When the moving platform moves, the actuator force  $f$  has the relation with the external force or torque  $F$  as follows:

$$J^T f = F. \quad (16)$$

There exist unitary matrices  $U$  and  $V$  which have the following equation

$$U^H J V = \begin{bmatrix} \sum 1 & 0 \\ 0 & 0 \end{bmatrix}, \quad (17)$$

where  $\sum 1 = \text{diag}(\sigma_1, \dots, \sigma_r)$ ,  $\sigma_1 \geq \dots \geq \sigma_r > 0$ ,  $r$  is the rank of the Jacobian matrix, then one can have  $\sigma_{\max} = \sigma_1$ ,  $\sigma_{\min} = \sigma_r$ , furthermore, one has the following:

$$(\det(J^T J))^{1/2} = \prod_{i=1} \sigma_i \quad (18)$$

where  $\sigma_i$  can be seen as the value of magnification of output speed to input speed. According to above equation, when the external force or torque exerted on the moving platform is constant and  $(\det(J^T J))^{1/2}$  is relative bigger and actuator force is relative smaller, that would be better for actuating the moving platform. The mechanism will be in the singular condition if  $(\det(J^T J))^{1/2} = 0$ . We define the following index to evaluate the driving force of the mechanism. The more the value is, the better performance of the mechanism has. The mechanism tends to get to the singular condition if the value is approaching 0.

$$D = (\det(J^T J))^{1/2} \quad (19)$$

Figure 11 shows the driving capacity index distribution when  $h$  is 0.6 m and the radii of the base and moving platform are 0.08 m and 0.03 m as a case. Similarly as above, through many different experiments, one can find that the driving force index ranges slightly in the workspace and properly distributed. Furthermore, the index doesn't change dramatically while the moving platform changes and the driving force index does not exist zero condition which means the mechanism does not exist singular conditions when the moving platform moves. The mechanism has good driving force performance as well.

### Conclusion

This paper mainly focuses on the stiffness, workspace and two dynamic performances analysis of 4UPS-PU mechanism. The inverse kinematic and Jacobian matrix of the mechanism were first derived. Secondly, we analyzed and optimized the global stiffness to obtain the optimal stiffness in each direction by using Genetic algorithm. Thirdly, the workspace of the 4UPS-PU mechanism was optimized by maximizing the global condition index derived by using Monte Carlo method to have the well-conditioned workspace without having the undesirable kinematics like poor dexterity. Finally, we focused on the driving force and loading capacity performance of the 4UPS-PU mechanism, through the analysis, one can see that the mechanism has good dynamic performances as a whole.

## References

- [1] D.Zhang, *Parallel robotic machine tools*. Springer. (2009).
- [2] N. Gorie, V. Dolga. Bio-mechatronics recovery systems for persons with disabilities. *Proceedings of International Conference On Innovations, Recent Trends And Challenges In Mechatronics, Mechanical Engineering And New High-Tech Products Development –MECAHITECH'11*, vol. 3. (2011)
- [3] G. Castelli, E. Ottaviano. Modeling, simulation and testing of a reconfigurable cable-based parallel manipulator as motion aiding system. *Applied Bionics and Biomechanics*, 7, 253-268. (2010)
- [4] M. Pan. Improved design of a three-degree of freedom hip exoskeleton based on biomimetic parallel structure. Dissertation for Master Degree. University of Ontario Institute of Technology, Canada. (2011)
- [5] H.J. Yu. Research on parallel robot based flexible fixtures for automotive. Ph.D thesis, China: Harbin Institute of Technology, (2010).
- [6] L.W. Tsai, S. Joshi. Kinematics and optimization of a spatial 3-UPU parallel manipulator. *Journal of Mechanical Design*, vol.122, p.439-446. (2000)
- [7] L.W. Tsai, S. Joshi. Kinematic analysis of 3-DOF position mechanisms for use in hybrid kinematic machines. *Journal of Mechanical Design*, vol.124, p.245-253. (2002)
- [8] D. Zhang, C.M. Gosselin. Kinetostatic modeling of N-DOF parallel mechanisms with a passive constraining leg and prismatic actuators, *Journal of Mechanical Design*, vol.123, p.375-381. (2001)
- [9] D. Zhang. Kinetostatic analysis and optimization of parallel and hybrid architecture for machine tools. Ph.D.thesis, Laval University, Canada. (2000)
- [10] Y.M. Li, Q.S. Xu. Stiffness analysis for a 3-PUU parallel kinematic machine. *Mechanism and Machine Theory*, p. 186-200. (2008)
- [11] T. Huang, J.S. Wang, D.J. Whitehouse. Closed form solution to the position workspace of Stewart parallel manipulators, *Science in China, Series E: Technological Sciences*, 41 (4), p.394–403. (1998)
- [12] J. Wang. Workspace evaluation and kinematic calibration of Stewart platform. Ph.D thesis, Florida Atlantic University. (1992).
- [13] J.Z. Jin. Analysis and simulation of the parallel manipulator workspace. Dissertation for Master Degree. Yanshan University. (2009)
- [14] J.M. Luo. Study on the structural synthesis about the partly-DOF parallel robot mechanisms and constraint chains. Ph.D thesis, Northeastern University. (2006).
- [15] X.L. Hu. Design and analysis of a three degrees of freedom parallel kinematic machine. Dissertation for Master Degree. University of Ontario Institute of Technology, Canada. (2008)
- [16] D. Zhang, Z.M. Bi, B.Z. Li. Design and kinetostatic analysis of a new parallel manipulator. *Robotics and Computer-Integrated Manufacturing*, 25, p.782-791.(2009)
- [17] R.E. Stamper, L.W. Tsai, G.C. Walsh. Optimization of a three DOF translational platform for well-conditioned workspace. *Proceedings of the IEEE International Conference on Robotics and Automation*, New Mexico, USA, 3250-3255. (1997)
- [18] G.H. Cui, Q.C. Li, Y.W. Zhang, H.J. Hou. Dynamic performance indices analysis of

4-SPS-1-S spatial rotation parallel manipulator. *Transactions of the Chinese Society for Agricultural Machinery*. 41(7). (2010)

Wei Bin  
Hebei University of Engineering  
Department of Equipment Manufacturing  
199 Guangming South Street  
Handan, 056038, Hebei Province, China  
[brave.1987@163.com](mailto:brave.1987@163.com)